RSC Advances

PAPER

View Article Online
View Journal | View Issue

Cite this: *RSC Adv.*, 2016, **6**, 20901

Surface functionalization of chitosan isolated from shrimp shells, using salicylaldehyde ionic liquids in exploration for novel economic and ecofriendly antibiofoulants†

Reda F. M. Elshaarawy,*[ab] Fatma H. A. Mustafa,[c] Annika Herbst,[b] Aida E. M. Farag[d] and Christoph Janiak[b]

Received 22nd December 2015
Accepted 25th January 2016

DOI: 10.1039/c5ra27489c

www.rsc.org/advances

Since the use of organotin as antifouling additives was prohibited in 2003, many researchers have endeavored to design and develop novel economic environment-friendly marine antifouling additives. This work reports the successful functionalization of biopolymeric chitosan, isolated from shrimp shells, with salicylidene ionic liquid (IL-Sal) brushes, (ILCSB**1–6**). These designed architectures were structurally and morphologically characterized. Marine biofouling-inducing bacterial strains (*S. aureus*, *E. coli*, *A. hydrophila* and *Vibrio*) were selected as microfoulants for a laboratory antibacterial and biofilm susceptibility assay investigation. Our outcomes unveiled a novel promising ecofriendly biocidal agent with excellent and broad antibacterial efficacy compared to parent chitosan and the standard antifoulant, Diuron®. The fabricated poly-IL-brushes chitosan architectures were subjected to a rigorous test in a field trial in Red Sea water. Our findings provide new insights into eco-friendly antifouling additives as an alternative to traditional antifouling agents. Novel IL-functionalized chitosan-based coatings exhibited long-term durability, surface inertness and promising antifouling performance.

Introduction

The invasive biofouling process is a source of serious negative environmental and economic impact that creates adverse influences on marine-related activities, metal-based materials, medicinal implants and also becomes the major drawback that limits the application of membrane filtration technology in wastewater treatment.[1] Bacteria are one of the major contributors to biofouling. Bacterial adhesion to a suitable surface or substrate is a crucial step in biofilm formation, which can ultimately allow colonization by macrofouling organisms.[2] For example, *Escherichia coli* (*E. coli*) and *Staphylococcus aureus* (*S. aureus*) are responsible for biofouling of fabric and medical devices[3] and their pronounced influence on marine bio-fouling was reported.[4] Additionally, it was reported that the marine-sourced bacteria (*Aeromonas* sp. and *Vibrio* sp.) were found to be essential for building up bacterial biofilms as a precursor for marine biofouling.[5]

To address surface biofouling while maintaining the bulk properties of the materials used, metal-based biofouling-fighting coatings (such as copper(I) compounds and organotins) have been developed[1,6] and used for a long time. However due to their acute harmful effects to the environment and non-target organisms, they were recently banned by IMO (International Maritime Organization).[7]

Thus, it remains one of the most important challenges is to develop environmentally friendly antifoulants with synergistic antibacterial efficacy, which could be further incorporated into the matrix of commercial coatings to obtain safe ecofriendly antibacterial/antibiofouling coatings for a variety of applications.

To date, the natural biopolymer chitosan (CS), an amino-glucopyranans heteropolymer composed of *N*-acetylglucosamine (GlcNAc) and glucosamine ($GlcNH_2$) units, may offer an ideal promising candidate for antibiofoulants due to its broad antimicrobial (antibacterial, antifungal, anti-algal) efficacy[8] and excellent antifouling[9] profile. Furthermore, chitosan could be part of a green chemistry approach to fight biofouling as chitosan is extracted mainly from marine organism by-products (*e.g.* shrimp shell) using very simple methods (*i.e.* economically attractive).

[a]*Faculty of Science, Suez University, Suez, Egypt. E-mail: reda_elshaarawi@science.suez.edu.eg; Reda.El-Shaarawy@uni-duesseldorf.de*

[b]*Institut für Anorganische Chemie und Strukturchemie, Heinrich-Heine Universität Düsseldorf, 40204 Düsseldorf, Germany. E-mail: janiak@uni-duesseldorf.de*

[c]*National Institute of Oceanography and Fisheries (NIOF), Marine Environment Division, Suez, Egypt*

[d]*National Institute of Oceanography and Fisheries (NIOF), Marine Biotechnology and Natural Products Extraction, Alexandria, Egypt*

† Electronic supplementary information (ESI) available: Experimental and spectral data. See DOI: 10.1039/c5ra27489c

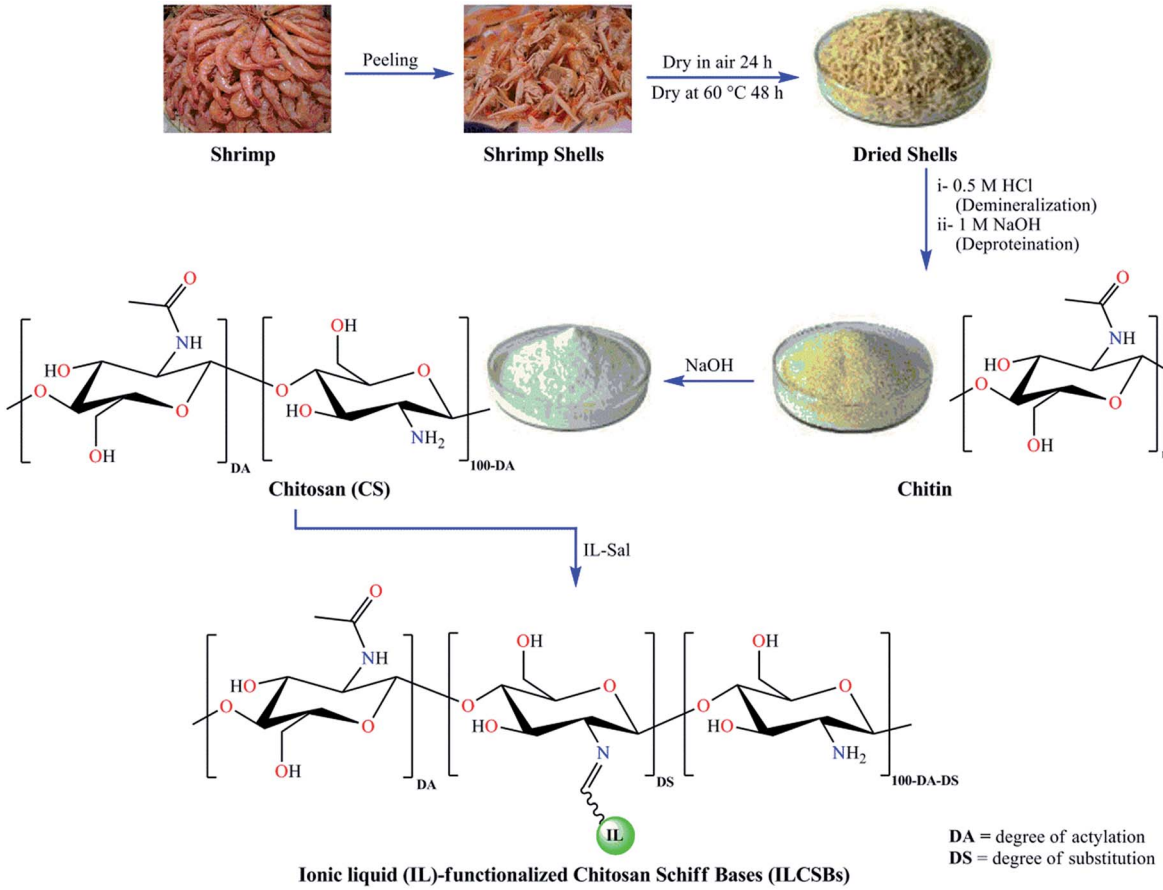

Scheme 1 Schematic representation of the extraction of chitosan from shrimp shells and synthetic route to ionic liquid-based chitosan Schiff bases.

It is well known that quaternary ammonium salts exhibit high biocidal activity due to their strong electrostatic interaction with the anionic microbial cell wall[10] followed by diffusion and disruption of the cytoplasmic membrane causing leakage of microorganism constituents and finally cell death.[11] Interestingly, antimicrobial susceptibility assays of imidazolium, pyridinium and quaternary ammonium ionic liquid (IL)-based architectures demonstrated significantly higher activities.[12] Notably, many ionic liquids display biocidal activity against Gram-positive/-negative bacteria, fungi and algae.[13]

Recently, much attention has thus been paid to polymeric ionic liquids (PILs) due to their interesting properties, such as high thermal stability, inherent conductivity,[14] excellent mechanical and electrochemical properties,[15] biocompatibility, and as good matrices for enzyme immobilization,[16] as well as promising precursors for catalytic membranes.[17]

To the best of our knowledge, there are no reports about the design and fabrication of polymeric ionic liquid-based chitosan Schiff bases (ILCSBs) (see Scheme 1) for antifouling evaluation. Inspired by previously mentioned facts and in continuation of our ongoing programs directed toward the development of novel materials for biological application,[12a–c,18] we aimed herein to explore the antibacterial and antibiofouling profiles of novel PILs-based chitosan architectures in search of developing a new economically attractive/ecofriendly promising antibiofoulants.

Experimental section

Instrumentation, materials and preparation details of a series of salicylaldehydes ionic liquids can be found in the ESI.† Elemental analysis data of CS and ILCSBs is given in Table 1 and used in the Results and discussion section to derive at molecular formulas for these compounds.

Extraction of chitin from shrimp shells

As a literature survey shows,[19] the following conditions were chosen as an optimal extractive treatment: the first stage of the extraction process involves a thermomechanical treatments, where the shells are scraped free of loose tissue and washed individually in lightly saline water, then separated from cephalothoraxes, salted (5 kg of NaCl per 250 g of shell), washed thoroughly in distilled water, dried in the sun (25–30 °C) for 3 days, and finally dried in an oven at 60 °C for 48 h. After that, the dried shells were grinded, sieved, and the fraction below 80 μm was used hereafter. The second stage started with a demineralization process which was carried out using 0.5 M HCl solutions. Typically, 100 g of shrimp shells powder was immersed in

Table 1 DS and proposed molecular formula of monomeric unit with elemental analysis for chitosan and ILCSBs

Sample	DA[a] (%)	DS[b] (%)	Molecular formula of monomeric unit (M, g mol^{-1})	EA calcd (found) (%)		
				C	H	N
CS	24.3	—	$(C_8H_{13}NO_5)_{0.243}(C_6H_{11}NO_4)_{0.757}\cdot H_2O$ (189.39)	41.13 (40.63)	7.18 (7.12)	7.18 (7.31)
ILCSB**1**	—	51.8	$(C_8H_{13}NO_5)_{0.243}(C_6H_{11}NO_4)_{0.239}(C_{18}H_{23}ClN_3O_5)_{0.518}$ (293.77)	51.99 (52.35)	6.08 (6.33)	9.72 (9.92)
ILCSB**2**	—	49.4	$(C_8H_{13}NO_5)_{0.243}(C_6H_{11}NO_4)_{0.263}(C_{20}H_{32}ClN_2O_5)_{0.494}$ (297.34)	54.16 (53.92)	7.41 (7.54)	7.04 (7.02)
ILCSB**3**	—	50.3	$(C_8H_{13}NO_5)_{0.243}(C_6H_{11}NO_4)_{0.258}(C_{20}H_{24}ClN_2O_6)_{0.503}$ (303.03)	53.53 (53.17)	5.99 (6.21)	6.94 (7.26)
ILCSB**4**	—	50.8	$(C_8H_{13}NO_5)_{0.243}(C_6H_{11}NO_4)_{0.249}(C_{18}H_{23}F_6N_3O_5P)_{0.508}$ (346.60)	43.58 (43.76)	5.11 (5.21)	8.14 (7.78)
ILCSB**5**	—	47.1	$(C_8H_{13}NO_5)_{0.243}(C_6H_{11}NO_4)_{0.286}(C_{20}H_{32}F_6N_2O_5P)_{0.471}$ (342.80)	45.81 (45.49)	6.28 (6.35)	6.01 (5.84)
ILCSB**6**	—	49.1	$(C_8H_{13}NO_5)_{0.243}(C_6H_{11}NO_4)_{0.265}(C_{20}H_{24}F_6N_2O_6P)_{0.491}$ (354.21)	45.31 (44.96)	5.09 (5.14)	5.90 (5.73)

[a] DA = degree of acetylation. [b] DS = degree of substitution.

1000 mL of 0.5 M HCl at ambient temperature (25 °C) under constant stirring for 24 h. After filtration, the residue was washed with distilled water until the pH of the rinsed water became neutral. Then the residue was subjected to deproteination, by immersing in 1000 mL of 1 M NaOH under vigorous stirring at 60 °C for 24 h. Then the proteins were removed by filtration. Distilled water was used to wash the residue to neutral. Then, the shrimp shell residue was subjected to the above procedure, starting with the thermochemical treatment, two more times. The chitin obtained still had a slight pink colour. Further decolourisation was achieved by soaking chitin in 250 mL of 1% $KMnO_4$ for 1 h. Followed by 250 mL of 1% oxalic acid for 2 h. The amount of 250 mL of 95% ethanol and 200 mL of absolute ethanol were sequentially used to remove ethanol-soluble substances from the obtained crude chitin and to dehydrate the chitin. Finally the chitin was dried in air at 50 °C overnight. Yield 96.34 g (96.34% based on 100 g of shrimp shell powder).

Preparation of chitosan (CS)

The purified chitin was deacetylated to form chitosan by treating 10 g of chitin with 100 mL 65% NaOH under stirring at 60 °C for 72 h. After filtration, the residue was washed three times with 10 mL of hot deionized water at 60 °C. The crude chitosan (7.9 g) was obtained by drying in an air oven at 50 °C overnight. The obtained crude chitosan was purified by dissolution in 1% (v/v) aqueous acetic acid until a homogenous solution is obtained, filtered through 22 μm Whatman filter paper to remove insoluble impurities, then precipitated by titration with 1 N NaOH until pH value of 8.5, and finally washed several times with distilled water. Yield 7.5 g (92.6% based on chitin). FTIR (KBr, cm^{-1}): 3462 (m, br, $\nu_{(O-H+NH_2)}$), 3101 (m, br, $\nu_{(N-H)}$), 1653 (vs, sh, $\nu_{(C=O)acetyl}$), 1568 (m, sh, amide II), 1380 (m, sh, amide III), 1069 (m, sh, $\nu_{(C-O-C)str}$), 896 (m, sh, $\nu_{(C-O-C)}$, β-glycosidic linkage). ^{1}H NMR (600 MHz, 1% $CD_3COOD/D_2O)_{60\ °C}$ δ (ppm): 5.22 (d, J = 7.2 Hz, 1H, $GlcNH_2$ residue), 4.24 (m, 2H, $GlcNH_2$ and GlcNAc residue), 4.12–3.90 (m, 3H, $GlcNH_2$ and GlcNAc residue), 3.53 (s, 1H, $GlcNH_2$ residue), 2.40 (s, 3H, NHAc). ^{13}C NMR (151 MHz, 1% $CD_3COOD/D_2O)_{60\ °C}$ δ (ppm): 177.03, 98.16, 94.35, 90.46, 83.89, 75.27, 70.73, 68.57, 62.80, 60.53, 56.28, 46.01, 32.61 and 23.54. Degree of acetylation 24.3%. Anal. calcd for $(C_8H_{13}NO_5)_{0.243}(C_6H_{11}NO_4)_{0.757}\cdot H_2O$ (M = 189.39 g mol^{-1}): C, 41.13; H, 7.18; N, 7.18; found C, 40.63; H, 7.12; N, 7.31. For SEM images see Fig. 4.

Synthesis of the salicylaldehyde ionic liquid (IL-Sal)-functionalized chitosan Schiff bases (ILCSB1–6)

A portion of 1 g of CS was dissolved in 200 mL of a mixed solution of 1% aqueous acetic acid (100 mL) and ethanol (100 mL) under stirring at room temperature for 30 min. Ionic liquid-based salicylaldehyde (IL-Sal, **2**, **3a–c**, see ESI† for synthesis) (equivalent to the molar N-content in CS) was dissolved in EtOH (30 mL) and the solution was added to the chitosan solution over a period of 30 min at 30 °C. Then the reaction mixture was stirred at 40 °C for 24 h. The reaction product was precipitated by adding an excessive amount of ethyl acetate (AcOEt) under ultrasonic irradiation at r.t. for 3 h, filtered to remove the solvent and then washed with 3 × 10 mL of 30 : 70, 20 : 80, and 0 : 100 EtOH : AcOEt mixtures sequentially. Finally, the product was dried at 35 °C under vacuum for 24 h to obtain the desired ionic liquids-functionalized chitosan Schiff bases (ILCSB**1–6**).

5-(1-Methylimidazol-3-ium chloride)-salicylidene chitosan (ILCSB1). Canary yellow powder, yield (1.53 g, 98.6%). FTIR (KBr, cm^{-1}): 3424 (vs, br, $\nu_{(O-H+NH_2)}$), 3147 (m, br, $\nu_{(N-H)}$), 1659 (vs, sh, $\nu_{(C=O)acetyl}$), 1635 (vs, sh, $\nu_{(C=N)azomethine}$), 1562 (m, sh, amide II), 1369 (m, sh, amide III), 1285 (m, sh, $\nu_{(Ar-O)}$), 1155 (s, sh, $\nu_{(H-C=C+H-C=N)bend}$, Im), 1063 (m, sh, $\nu_{(C-O-C)str}$), 895 (m, sh, $\nu_{(C-O-C)}$, β-glycosidic linkage), 760 (m, sh, Im). ^{1}H NMR (600 MHz, 1% $CD_3COOD/D_2O)_{60\ °C}$ δ (ppm): 10.35 (s, 1H, OH), 10.29 (s, 1H, OH), 9.07 (d, J = 11.7 Hz, 2H, 2 × H–C=N), 8.14 (s, 1H, NH of GlcNHAc residue), 8.10 (d, J = 9.0 Hz, 1H, Ar-H), 7.98 (dd, J = 8.8, 2.4 Hz, 2H, 2 × Ar-H), 7.90–7.72 (m, 2H, 2 × Ar-H), 7.60–7.39 (m, 1H, Ar-H), 5.75 (s, 2H, CH_2 of CH_2Ar), 5.24 (s, 1H,

GlcN residue), 4.25 (s, 6H, 2 × CH_3 of MeIm), 3.84 (t, J = 7.2 Hz, 5H, GlcN and GlcNHAc residue), 3.56 (s, 1H, GlcN residue), 3.17 (br, s, 6H, GlcN and GlcNHAc residue), 2.76 (t, J = 8.2 Hz, 2H, GlcN and GlcNHAc residue), 2.40 (tt, J = 15.4, 7.4 Hz, 3H, NHAc). ^{13}C NMR (151 MHz, 1% $CD_3COOD/D_2O)_{60\ °C}$ δ (ppm): 177.14, 168.29, 155.10, 153.27, 141.89, 137.77, 133.84, 126.20, 124.50, 122.66, 118.78, 111.90, 101.96, 98.53, 88.15, 84.77, 70.65, 61.16, 57.76, 50.71, 45.27, 42.29, 38.72, 36.27, 31.22, 29.79 and 22.51.

5-(*N*,*N*,*N*-Triethylammonium chloride)-salicylidene chitosan (ILCSB2). Yellow crystals, yield (1.54 g, 98.1%). FTIR (KBr, cm^{-1}): 3451 (vs, br, $\nu_{(O-H+NH_2)}$), 3150 (m, br, $\nu_{(N-H)}$), 1661 (s, sh, $\nu_{(C=O)acetyl}$), 1638 (vs, sh, $\nu_{(C=N)azomethine}$), 1556 (m, sh, amide II), 1377 (m, sh, amide III), 1283 (m, sh, $\nu_{(Ar-O)}$), 1073 (m, sh, $\nu_{(C-O-C)str}$), 896 (m, sh, $\nu_{(C-O-C)}$, β-glycosidic linkage). ^{1}H NMR (600 MHz, 1% $CD_3COOD/D_2O)_{60\ °C}$ δ (ppm): 10.35 (s, 2H, 2 × OH), 9.08 (d, J = 11.9 Hz, 2H, 2 × H–C═N), 8.24 (d, J = 11.9 Hz, 1H, NH of GlcNHAc residue), 8.14 (d, J = 2.4 Hz, 1H, Ar-H), 7.98 (d, J = 8.7 Hz, 1H, Ar-H), 7.86–7.80 (m, 3H, 3 × Ar-H), 7.47 (d, J = 8.7 Hz, 1H, Ar-H), 5.77 (s, 4H, 2 × CH_2 of CH_2Ar), 5.27 (d, J = 7.3 Hz, 1H, GlcN residue), 4.28–4.22 (m, 6H, GlcN and GlcNAc residue), 4.11 (s, 2H, GlcNAc residue), 3.84 (t, J = 7.2 Hz, 4H, 2 × CH_2), 3.56 (br, s, 2H, GlcN residue), 3.39–3.29 (q, 6H, 3 × CH_2 of $\mathbf{CH_2}CH_3$), 3.15–2.94 (q, 6H, 3 × CH_2 of $\mathbf{CH_2}CH_3$), 2.76 (t, J = 8.2 Hz, 4H, GlcN and GlcNHAc residue), 2.43–2.34 (br, m, 3H, CH_3, NHAc), 2.12–2.01 (t, J_{HH} = 7.00 Hz, 9H, 3 × $CH_2\mathbf{CH_3}$), 1.88–1.76 (t, J_{HH} = 7.02 Hz, 9H, 3 × $CH_2\mathbf{CH_3}$). ^{13}C NMR (151 MHz, 1% $CD_3COOD/D_2O)_{60\ °C}$ δ (ppm): 177.21, 164.30, 159.57, 138.23, 135.13, 133.42, 126.51, 124.22, 122.73, 119.08, 107.34, 100.21, 83.89, 77.61, 76.55, 72.36, 66.19, 61.28, 56.91, 53.65, 50.48, 36.97, 31.99, 29.78, 23.66, 17.89.

5-(2-Methoxypyridinium chloride)-salicylidene chitosan (ILCSB3). Pale yellow powder, yield (1.58 g, 98.7%). FTIR (KBr, cm^{-1}): 3436 (vs, br, $\nu_{(O-H+NH_2)}$), 3158 (m, br, $\nu_{(N-H)}$), 1656 (s, sh, $\nu_{(C=O)acetyl}$), 1640 (vs, sh, $\nu_{(C=N)azomethine}$), 1524 (m, sh, amide II), 1373 (m, sh, amide III), 1286 (m, sh, $\nu_{(Ar-O)}$), 1159 (s, sh, $\nu_{(H-C=C+H-C=N)bend}$, Py), 1070 (m, sh, $\nu_{(C-O-C)str}$), 897 (m, sh, $\nu_{(C-O-C)}$, β-glycosidic linkage), 769, 657 (m, sh, Py^+). ^{1}H NMR (600 MHz, 1% $CD_3COOD/D_2O)_{60\ °C}$ δ (ppm): 10.35 (s, 1H, OH), 10.27 (s, 1H, OH), 8.99 (dd, J = 18.4, 7.4 Hz, 2H, 2 × H–C═N), 8.24 (d, J = 7.5 Hz, 1H, Py), 8.15 (d, J = 7.3 Hz, 1H, NH of GlcNHAc residue), 8.00 (d, J = 8.7 Hz, 1H, Py), 7.81 (dd, J = 26.5, 7.5 Hz, 4H, Py + Ar), 7.59 (t, J = 7.7 Hz, 1H, Ar), 7.48 (d, J = 8.7 Hz, 1H, Ar), 5.98 (s, 4H, 2 × CH_2 of CH_2Ar), 5.25 (d, J = 7.7 Hz, 1H, GlcN residue), 4.48 (s, 6H, 2 × CH_3 of MeOPy), 4.27 (br, s, 2H, GlcN and GlcNHAc residue), 4.15–4.00 (br, m, 4H, GlcN and GlcNHAc residue), 3.83 (t, J = 7.2 Hz, 2H, GlcN residue), 3.56 (br, s, 2H, GlcN residue), 3.27–3.14 (br, m, 4H, GlcN and GlcNHAc residue), 2.76 (t, J = 8.1 Hz, 2H, GlcNHAc residue), 2.40 (dd, J = 15.6, 8.6 Hz, 3H, NHAc). ^{13}C NMR (151 MHz, 1% $CD_3COOD/D_2O)_{60\ °C}$ δ (ppm): 177.10, 172.20, 166.91, 163.00, 156.50, 145.76, 140.02, 137.85, 134.09, 125.86, 122.05, 118.99, 114.19, 113.77, 91.88, 81.51, 73.45, 71.10, 68.34, 62.06, 58.38, 56.41, 53.48, 50.71, 42.36, 31.21, 17.54, 13.93.

5-(1-Methylimidazol-3-ium hexafluorophosphate)-salicylidene chitosan (ILCSB4). Yellow powder, yield (1.81 g, 98.9%). FTIR (KBr, cm^{-1}): 3431 (vs, br, $\nu_{(O-H+NH_2)}$), 3145 (m, br, $\nu_{(N-H)}$), 1660 (s, sh, $\nu_{(C=O)acetyl}$), 1634 (vs, sh, $\nu_{(C=N)azomethine}$), 1558 (m, sh, amide II), 1370 (m, sh, amide III), 1285 (m, sh, $\nu_{(Ar-O)}$), 1155 (s, sh, $\nu_{(H-C=C+H-C=N)bend}$, Im), 1066 (m, sh, $\nu_{(C-O-C)str}$), 895 (m, sh, $\nu_{(C-O-C)}$, β-glycosidic linkage), 836 (s, sh, $\nu_{(PF_6^-)}$), 761 (m, sh, Im). ^{1}H NMR (600 MHz, 1% $CD_3COOD/D_2O)_{60\ °C}$ δ (ppm): 10.35 (s, 1H, OH), 10.28 (s, 1H, OH), 9.06 (d, J = 11.5 Hz, 2H, 2 × H–C═N), 8.17 (s, 1H, NH of GlcNHAc residue), 8.10 (d, J = 8.7 Hz, 1H, Ar-H), 7.96 (dd, J = 8.5, 2.1 Hz, 2H, 2 × Ar-H), 7.89–7.75 (m, 2H, 2 × Ar-H), 7.61–7.42 (m, 1H, Ar-H), 5.76 (s, 4H, 2 × CH_2 of CH_2Ar), 5.25 (s, 1H, GlcN residue), 4.25 (s, 6H, 2 × CH_3 of MeIm), 3.85 (t, J = 7.0 Hz, 5H, GlcN and GlcNHAc residue), 3.53 (s, 1H, GlcN residue), 3.16 (br, s, 6H, GlcN and GlcNHAc residue), 2.76 (t, J = 8.2 Hz, 2H, GlcN and GlcNHAc residue), 2.40 (m, 3H, NHAc). ^{13}C NMR (151 MHz, 1% $CD_3COOD/D_2O)_{60\ °C}$ δ (ppm): 176.24, 168.56, 154.95, 152.87, 141.89, 138.02, 133.84, 126.22, 124.51, 122.53, 118.89, 111.90, 102.12, 98.13, 87.25, 84.48, 70.65, 61.61, 57.32, 50.71, 45.26, 41.99, 38.72, 35.87, 31.22, 30.13, 22.56.

5-(*N*,*N*,*N*-Triethylammonium hexafluorophosphate)-salicylidene chitosan (ILCSB5). Yellow plates, yield (1.79 g, 98.8%). FTIR (KBr, cm^{-1}): 3425 (vs, br, $\nu_{(O-H+NH_2)}$), 3163 (m, br, $\nu_{(N-H)}$), 1659 (s, sh, $\nu_{(C=O)acetyl}$), 1633 (vs, sh, $\nu_{(C=N)azomethine}$), 1561 (m, sh, amide II), 1373 (m, sh, amide III), 1280 (m, sh, $\nu_{(Ar-O)}$), 1067 (m, sh, $\nu_{(C-O-C)str}$), 836 (s, sh, $\nu_{(PF_6^-)}$). ^{1}H NMR (600 MHz, 1% $CD_3COOD/D_2O)_{60\ °C}$ δ (ppm): 10.37 (s, 1H, ×OH), 10.28 (s, 1H, OH), 9.08 (d, J = 10.8 Hz, 2H, 2 × H–C═N), 8.26 (br, s, 1H, NH of GlcNHAc residue), 8.13 (d, J = 2.2 Hz, 1H, Ar-H), 7.98 (d, J = 8.7 Hz, 1H, Ar-H), 7.85–7.77 (m, 3H, 3 × Ar-H), 7.47 (d, J = 8.7 Hz, 1H, Ar-H), 5.75 (s, 4H, 2 × CH_2 of CH_2Ar), 5.26 (d, J = 7.3 Hz, 1H, GlcN residue), 4.28–4.23 (m, 6H, GlcN and GlcNAc residue), 4.21 (br, s, 2H, GlcNAc residue), 3.90 (t, J = 7.2 Hz, 4H, GlcN and GlcNAc residue), 3.63 (br, s, 2H, GlcN residue), 3.41 (q, 6H, 3 × CH_2 of $\mathbf{CH_2}CH_3$), 3.17 (q, 6H, 3 × CH_2 of CH_2CH_3), 2.76 (t, J = 8.2 Hz, 4H, GlcN and GlcNHAc residue), 2.40–2.34 (br, m, 3H, CH_3, NHAc), 2.03–1.92 (t, J_{HH} = 6.99, 7.01 Hz, 9H, 3 × $CH_2\mathbf{CH_3}$), 2.03–1.92 (t, J_{HH} = 7.15 Hz, 9H, 3 × $CH_2\mathbf{CH_3}$). ^{13}C NMR (151 MHz, 1% $CD_3COOD/D_2O)_{60\ °C}$ δ (ppm): 179.89, 166.93, 159.87, 139.36, 135.55, 134.27, 128.86, 125.74, 122.69, 120.83, 107.25, 100.99, 83.77, 77.23, 76.18, 72.07, 66.66, 61.50, 56.20, 53.31, 51.63, 36.79, 32.06, 30.13, 24.89, 18.92.

5-(2-Methoxypyridinium hexafluorophosphate)-salicylidene chitosan (ILCSB6). Yellowish white powder, yield (1.85 g, 98.9%). FTIR (KBr, cm^{-1}): 3438 (vs, br, $\nu_{(O-H+NH_2)}$), 3161 (m, br, $\nu_{(N-H)}$), 1655 (s, sh, $\nu_{(C=O)acetyl}$), 1637 (vs, sh, $\nu_{(C=N)azomethine}$), 1530 (m, sh, amide II), 1371 (m, sh, amide III), 1284 (m, sh, $\nu_{(Ar-O)}$), 1160 (s, sh, $\nu_{(H-C=C+H-C=N)bend}$, Py), 1070 (m, sh, $\nu_{(C-O-C)str}$), 898 (m, sh, $\nu_{(C-O-C)}$, β-glycosidic linkage), 840 (s, sh, $\nu_{(PF_6^-)}$). 769, 655 (m, sh, Py^+). ^{1}H NMR (600 MHz, 1% $CD_3COOD/D_2O)_{60\ °C}$ δ (ppm): 10.36 (s, 1H, OH), 10.27 (s, 1H, OH), 9.03 (d, J = 7.4 Hz, 2H, 2 × H–C═N), 8.24 (d, J = 7.5 Hz, 1H, Py), 8.14 (d, J = 7.2 Hz, 1H, NH of GlcNHAc residue), 7.98 (d, J = 8.7 Hz, 1H, Py), 7.80 (d, J = 7.5 Hz, 4H, Py + Ar), 7.55 (t, J = 7.6 Hz, 1H, Ar), 7.41 (d, J = 8.1 Hz, 1H, Ar), 5.88 (s, 4H, 2 × CH_2 of CH_2Ar), 5.23 (d, J = 7.7 Hz, 1H, GlcN residue), 4.45 (s, 6H, 2 × CH_3 of MeOPy), 4.27 (br, s, 2H, GlcN and GlcNHAc residue), 4.17–4.03 (br, m, 4H, GlcN and GlcNHAc residue), 3.82 (t, J = 7.0 Hz, 2H, GlcN residue), 3.54 (br, s, 2H, GlcNHAc residue), 3.18–3.00 (br,

m, 4H, GlcN and GlcNHAc residue), 2.75 (t, J = 8.1 Hz, 2H, GlcNHAc residue), 2.39 (d, J = 8.5 Hz, 3H, NHAc). ^{13}C NMR (151 MHz, 1% $CD_3COOD/D_2O)_{60\ ^\circ C}$ δ (ppm): 177.10, 174.60, 166.90, 162.65, 156.50, 145.77, 139.02, 137.64, 134.09, 125.86, 122.05, 118.99, 114.19, 113.77, 91.88, 81.51, 73.45, 71.10, 68.34, 62.06, 58.38, 56.41, 53.48, 51.68, 42.36, 32.21, 19.99, 17.98.

General procedure for the synthesis of films and solid powder samples

Thin films of CS or ILCSB were obtained by casting 3 mL of ionic liquid-functionalized biopolymer solution of CS or ILCSBs (0.1 g biopolymer/10 mL of 1% CH_3COOH) into a DUROPLAN Petri dish with diameter of 2.5 cm or 5 cm. The obtained crude films (Fig. 1) were further dried in vacuum at 35 °C. Powders of different yellow color intensities were also obtained by film grinding under liquid nitrogen. Samples of the isolated solids were characterized as shown in the Experimental section.

Anti-microfouling assays

Anti-bacterial activity against marine biofilm bacterial strains

Reagents. Dimethylsulphoxide (DMSO) and 3-(3,4-dichlorophenyl)-1,1-dimethylurea (Diuron®, DCMU) antifoulant ($C_9H_{10}Cl_2N_2O$, 233.09 g mol^{-1}) were obtained from Sigma Chemical Co. (Germany).

Bacterial cultures. The antibacterial activity of natural products was assessed against four bacterial species: *Staphylococcus aureus* ATCC 25923 (American Type Culture Collection, Rockville, MD), *Escherichia coli* ATCC 25922, *Aeromonas hydrophila*, and *Vibrio* maintained in BHI at 20 °C; 300 mL of each stock-culture were added to 3 mL of nutrient broth. Overnight cultures were kept for 24 h at 36 ± 1 °C and the purity of cultures was checked after 8 h of incubation. After 24 h of incubation, the bacterial suspension (inoculum) was diluted with sterile physiological solution, for the diffusion and indirect bioautographic tests, to 10^8 CFU mL^{-1} (turbidity = McFarland barium sulfate standard 0.5). For the direct bioautographic test, bacterial suspension was diluted with BHI broth to a density of approximately 10^9 UFC mL^{-1} (McFarland standard 3).

Antimicrobial susceptibility. Antimicrobial susceptibility of the bacterial strains was carried out by agar well diffusion method[20] for the target compounds as well as standard antifoulant, Diuron®. The diameter of the zones of inhibition (ZOI, mm) was measured accurately as indicative of antimicrobial activity.

Determination of MIC. As parameters of the antibacterial efficacy, the minimal inhibitory concentration (MIC) of the new compounds against marine bacterial isolates were determined using two different culture media: Mueller–Hinton broth and Luria Bertania (LB). The inoculum was prepared as described previously. ILCSBs products were dissolved in DMSO (10% of the final volume) and diluted with culture broth to a concentration of 2 mg mL^{-1}. Further 1 : 2 serial dilutions were performed by addition of culture broth to reach concentrations ranging from 2 to 0.0156 mg mL^{-1}; 100 μL of each dilution was distributed in 96-well plates, as well as a sterility control and a growth control (containing culture broth plus DMSO, without antimicrobial substance). Each tested and growth control wells were inoculated with 5 μL of a bacterial suspension (10^8 CFU mL^{-1} or 10^5 CFU per well). All experiments were performed in triplicate and the microdilution trays were incubated at 36 °C for 18 h. Bacterial growth was detected former by optical density (ELISA reader, CLX800-BioTek Instruments) and after by addition of 20 μL of an INT alcoholic solution (0.5 mg mL^{-1}) (Sigma). The trays were again incubated at 36 °C for 30 min, and in those wells, where bacterial growth occurred, INT changed from yellow to purple. MIC values were defined as the lowest concentration of each natural product, which completely inhibited microbial growth. The results were expressed in milligrams per milliliters using two different culture media: Mueller–Hinton broth and Luria Bertania (LB). The inoculum was prepared as described previously. Natural products were dissolved in DMSO (10% of the final volume) and diluted with culture broth to a concentration of 2 mg mL^{-1}. Further 1 : 2 serial dilutions were performed by addition of culture broth to reach concentrations ranging from 2 to 0.0156 mg mL^{-1}; 100 μL of each dilution were distributed in 96-well plates, as well as a sterility control and a growth control (containing culture broth plus DMSO, without antimicrobial substance). Each test and growth control well was inoculated with 5 μL of a bacterial suspension (10^8 CFU mL^{-1} or 10^5 CFU per well). All experiments were performed in triplicate and the microdilution trays were incubated at 36 °C for 18 h.

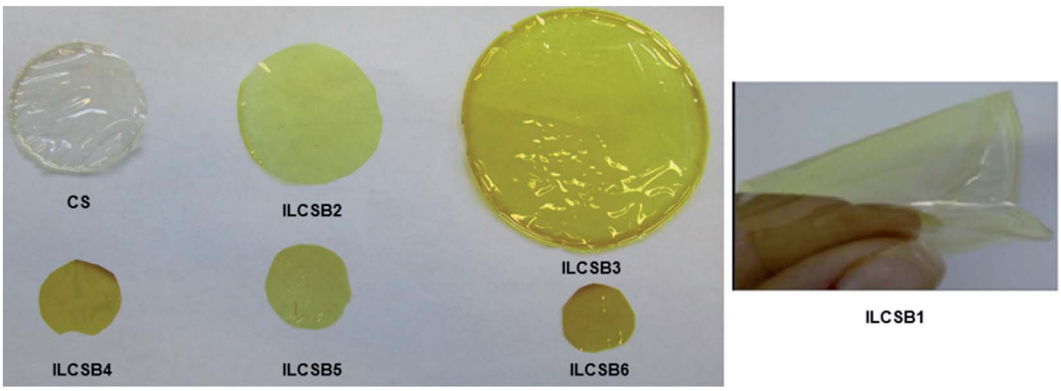

Fig. 1 Photographs of chitosan (CS) and ionic liquid salicidene (IL-Sal)-functionalized chitosan Schiff bases (ILCSBs**1–6**) biopolymeric films. The right image shows the flexibility of the films.

Bacterial growth was detected former by optical density (ELISA reader, CLX800-BioTek Instruments) and after by addition of 20 μL of an INT alcoholic solution (0.5 mg mL^{-1}) (Sigma). The trays were again incubated at 36 °C for 30 min, and in those wells, where bacterial growth occurred, INT changed from yellow to purple. MIC values were defined as the lowest concentration of each natural product, which completely inhibited microbial growth. The results were expressed in mg mL^{-1}.

Field anti-macrofouling assays at Eastern Harbor of Alexandria beach

Among novel polymeric ionic liquid-based chitosan Schiff bases, the most potent biocidal one, ILCSB**2**, has been selected to be subjected to a field immersion antifouling paint testing for monitoring its antifoulant properties over time under *in vivo* conditions. In this test; ILCSB**2** was mixed with an inert matrix using a suitable blend of resins and supporting it with nontoxic inert pigments to form a paint which was then immersed in the sea using suitable iron frames. Four marine paint formulations are prepared by incorporating ILCSB**2**, standard (Diuron®), chitosan extracted from shrimp shells and commercial chitosan bought from the market into soluble matrix paint, in addition to an inert paint formulation which used as a control. 0.2 mm thick sheets of acrylic were cut to panel dimensions of 10 × 15 × 0.2 cm (see Fig. 8). The panels were roughened using emery papers starting with a coarse one and proceeding in steps to finer grades. The panels were coated from front and back with two successive coats of the prepared paint, being allowed to dry for two days between each coating. The coated panels were connected to the tested frames with nylon threads through nails bored in the panels (see Fig. S1, ESI†). All panels were immersed in the Eastern Harbor of Alexandria, where their antifouling profiles were studied periodically from 12 May 2015 to 6 October 2015 by visual inspection and photographic recording (see Fig. 8). The condition of each coated panel was recorded as a total cover percentage with respect to different marine fouling organisms over different time intervals (see Fig. 9).

Results and discussion

Chemistry

In this work, dual quaternization strategy and Schiff-base chemistry have been used as a convenient route for surface functionalization of natural biopolymer chitosan (CS), which obtained by efficient deacetylation of chitin extracted from shrimp shells wastes (Scheme 2). The key starting materials ionic liquid salicylaldehydes (IL-Sal, **2**, **3a–c**) were synthesized starting from chloromethylsalicylaldehyde (**1**) *via* an efficient green chemistry protocol, in which, the chloromethylsalicylaldehyde was explored as agent for quaternization of various nitrogen-containing compounds (such as 1-methylimidazole (1-MeIm), triethylamine (Et_3N), 2-methoxypyridine (2-MeOPy)) to generate imidazolium/ammonium/pyridinium-based salicylaldehyde chlorides (**2a–c**), respectively. Anion metathesis of **2a–c** with hexafluorophosphoric acid ($HPF_{6(aq)}$) afforded the corresponding hexafluorophosphate salts (**3a–c**). Eventually, the desired ILCSB**1–6**, were obtained simply by Schiff-base condensation of ionic salicylaldehyde salts (**2**, **3a–c**) with the natural biopolymer chitosan. These chitosan architectures were isolated in excellent yields and structurally characterized by elemental analysis, FTIR, NMR (^1H, ^{13}C, ^{19}F, ^{31}P), as well as morphologically characterized by SEM analysis.

Structural characterizations of CS and ILCSBs

Structural characterizations of CS. The degree of acetylation (DA) was calculated from elemental analysis according to the following eqn (1):[21]

$$\begin{aligned} DA &= [(C/N - 5.14)/1.72] \times 100\% \\ &= [(40.63/7.31 - 5.14)/1.72] \times 100\% = 24.3\% \end{aligned} \quad (1)$$

Based on the elemental analysis and degree of deacetylation of chitosan, we propose a plausible structure for the monomeric building unit of CS in Scheme 3.

Spectral data (FTIR and NMR) provide further validation evidences for the proposed structure of the building block of CS. The FTIR spectral data of CS revealed an absorption peak for N–H stretching vibration of the NH_2 group, in $GlcNH_2$ at 3436 cm^{-1} and for the N–H stretching vibration of the NH group in GlcNHAc at ~3160 cm^{-1} coupled with an increase of NH_2 band intensity reflecting higher degree of deacetylation (*i.e.* higher $GlcNH_2$: GlcNHAc ratio). Stretches at 1653, 1568 and 1380 cm^{-1} are characteristic for carbonyl, amide II and amide III fragments of GlcNHAc. The FTIR spectra of commercial chitosan and chitosan obtained from shrimp shell were found to be quite similar. The degree of deacetylation (DDA) can be determined from the absorption or transmittance (*A* or *T*) ratios between C=O band ($A_{C=O}$), characteristic for *N*-acetylated fragment (GlcNHAc), and NH_2 band (A_{NH_2}), characteristic for *N*-deacetylated fragment ($GlcNH_2$), using the Kasaai eqn (2).[22]

$$DDA = 100 - \left(\frac{A_{C=O}}{A_{NH_2}} \times 115\right) = 100 - \left(\frac{A_{1653}}{A_{3462}} \times 115\right) \quad (2)$$

with here

$$A_{1653} = -\log(T_{1653}/100) = -\log(0.91144) = 0.04$$

and

$$A_{3462} = -\log(T_{3462}/100) = -\log(0.65010) = 0.19,$$

so that DDA = 75.8% and DA = 24.2% (in agreement with the value obtained from elemental analysis).

The degree of acetylation, DA of chitosan can also be calculated on the basis of proton signals intensities (*I*) assigned for H^1 or H^2, characteristic for $GlcNH_2$ fragment, and H^1 or CH_3, characteristic for GlcNHAc fragment, in the ^1H NMR spectra of CS (see Fig. 2) using one of the following eqn (3) and (4).[23]

$$DA\% = 100 - \frac{I_{H^1}}{I_{H^1} + (I_{CH_3}/3)} \times 100 \quad (3)$$

$$DA\% = 100 - \frac{I_{H^2}}{I_{CH_3}} \times 100 \quad (4)$$

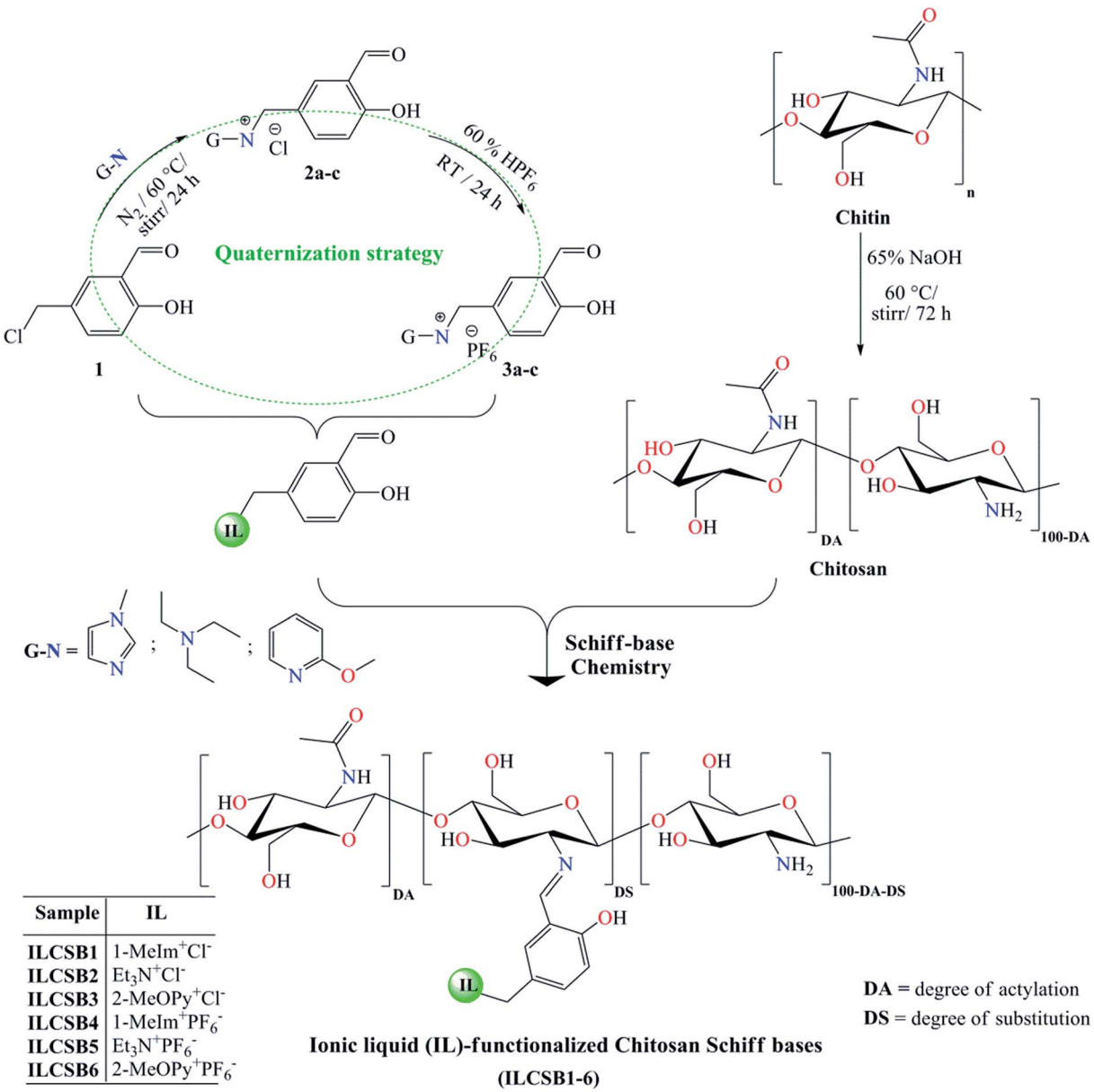

Scheme 2 Schematic diagram for the synthesis of ionic liquid salicylaldehydes (IL-Sal, **2**, **3a–c**) and surface-functionalized chitosan ILCSB**1–6**.

here I_{CH_3} = 1301.8, I_{H^1} = 756.4 and I_{H^2} = 985.1, so that the calculated value for DA% in using the 2nd equation is 24.3% which agrees with that calculated from EA and FTIR data.

In conclusion, elemental and spectral data for isolated chitosan from shrimp shells (of the degree of deacetylation (DDA) agree to ~75.7%) demonstrating that, the building block in CS architecture is a copolymer from $GlcNH_2$ and GlcNHAc kept at *ca.* 3 : 1 molar ratio, *i.e.*, $(GlcNHAc)_{0.243}(GlcNH_2)_{0.757}(H_2O)$ or $(C_8H_{13}NO_5)_{0.243}(C_6H_{11}NO_4)_{0.757}(H_2O)$ (fully agree with proposed structure *cf.* Scheme 3).

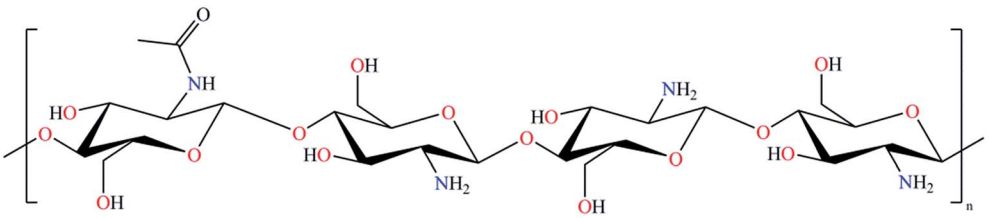

Scheme 3 Proposed structure for the monomeric building unit of CS.

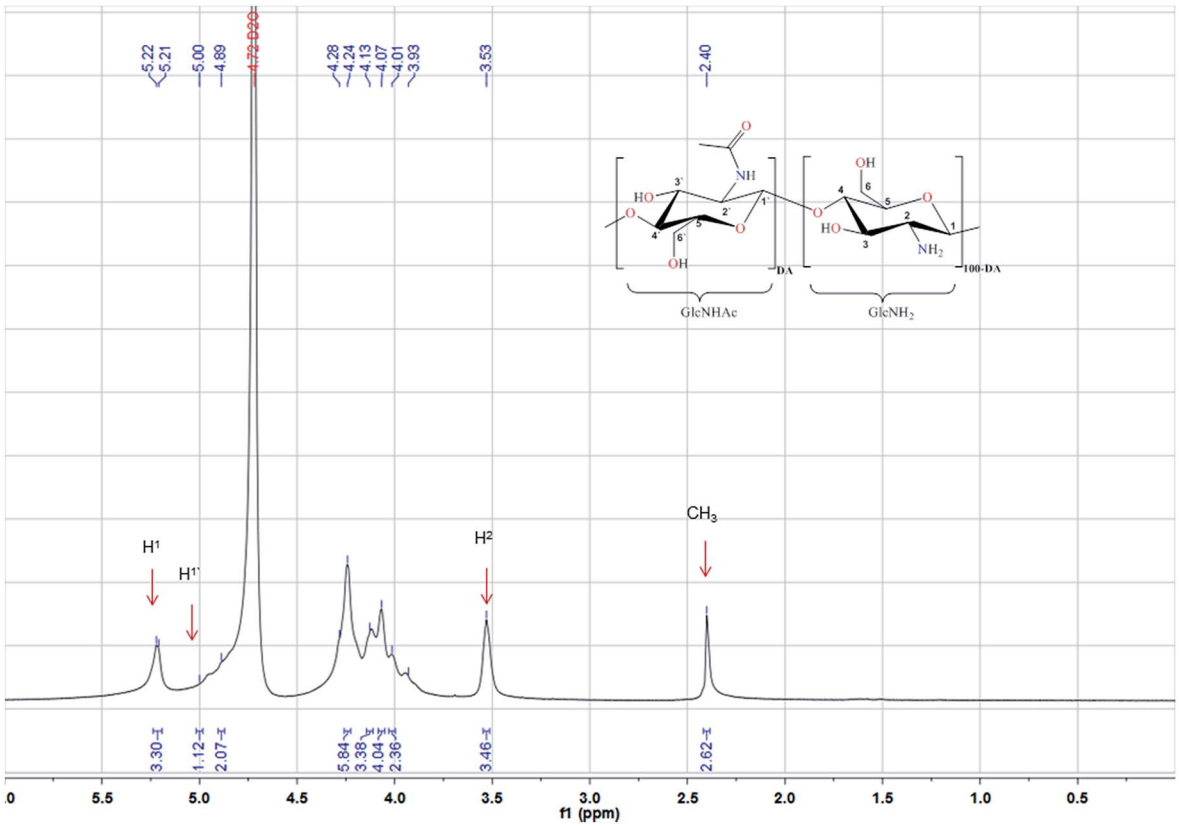

Fig. 2 ^{1}H NMR spectrum of CS (600 MHz, 1% CD_3COOD/D_2O 70 °C).

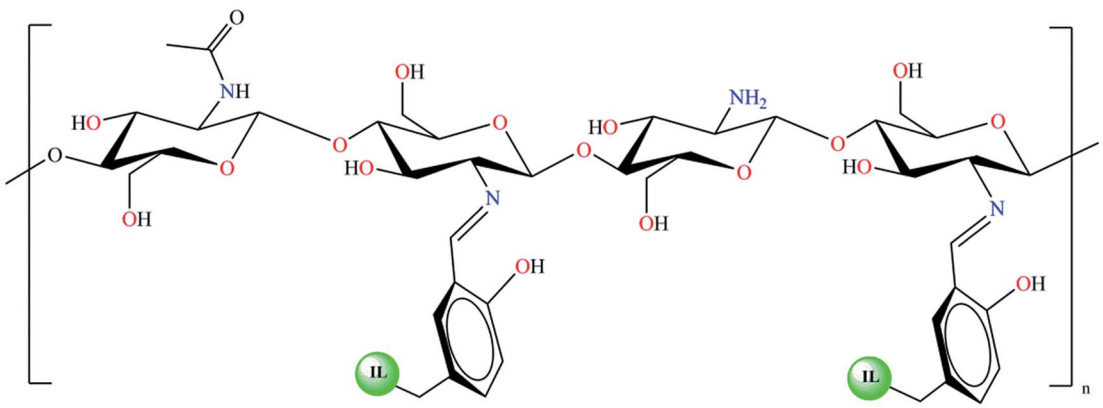

Scheme 4 Suggested structural formula for the building block of ILCSBs.

Structural characterizations of ILCSBs

Microanalytical data and degree of substitution DS (immunization) for ILCSBs. For synthesis of ILCSBs, the experimental conditions were optimized to avoid any loss of the final product during the reaction workup. Consequently, the obtained product yield could be used to calculate the degree of substitution DS (immunization) according to the following proposed reaction;

$$\underset{\text{CS}}{(C_8H_{13}NO_5)_{0.243}(C_6H_{11}NO_4)_{0.757}} + \underset{\mathbf{2},\ \mathbf{3a}-\mathbf{c}}{\text{ILsal}} \rightarrow \underset{\text{ILCSBs}(\mathbf{1}-\mathbf{6})}{(C_8H_{13}NO_5)_{0.243}(C_6H_{11}NO_4)_{0.757-x}(\text{ILsal}C_6H_9NO_4)_x}$$

x = degree of substitution (DS)

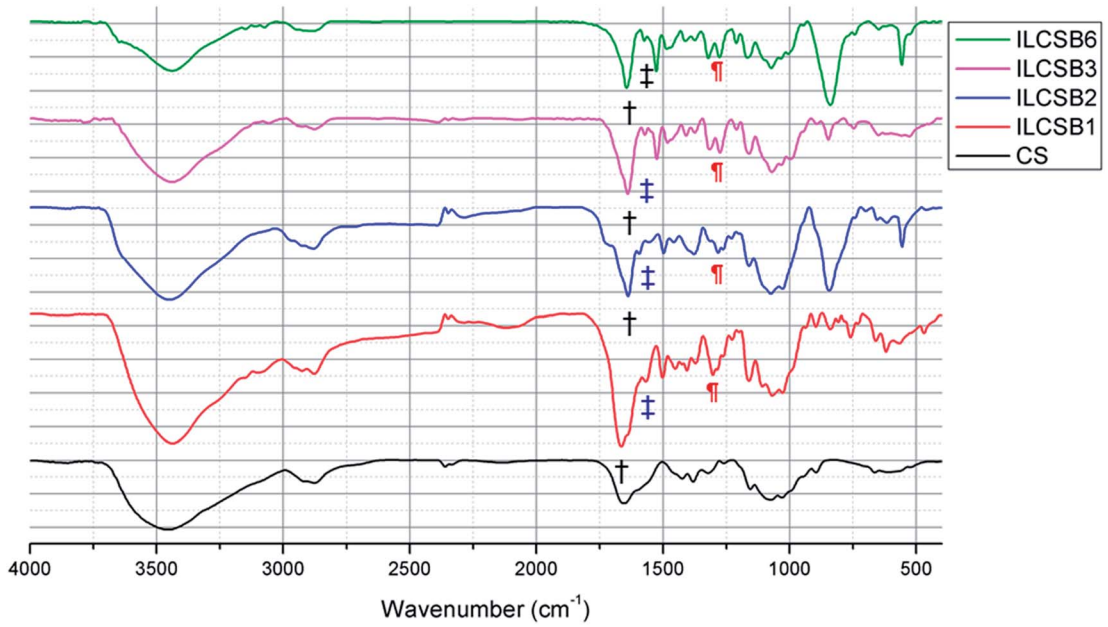

Fig. 3 FTIR patterns for comparison of the azomethine (H–C=N) stretching vibrations and splitting patterns of ILCSB**1–6** with CS. † = amide I stretch around 1660 cm^{-1}; ‡ = amine N–H stretch at *ca.* 1595 cm^{-1}; ¶ = aryl-O vibration bands at *ca.* 1285 cm^{-1}.

For example, Schiff-base condensation of chitosan (1.00 g) and **2a** yields 1.55 g of the ILCSB**1** product, *i.e.*, a 55% massive increase in chitosan weight. Consequently, the molecular weight of the monomeric building unit of ILCSB**1** will be 55% higher than the chitosan monomeric unit, *i.e.* $(C_8H_{13}NO_5)_{0.243}(C_6H_{11}NO_4)_{0.757}\cdot H_2O$ (M = 189.39 g mol^{-1}). The molecular weight of ILCSB**1** monomeric unit with an empirical formula of $(C_8H_{13}NO_5)_{0.243}(C_6H_{11}NO_4)_{0.757-x}(C_{18}H_{23}ClN_3O_5)_x$ will be 293.77 g mol^{-1}. By solving this equation, the value of DS is found to be 51.8% which is consistent with the values obtained from CHN analysis for ILCSB**1**. Anal. calcd for $(C_8H_{13}NO_5)_{0.243}(C_6H_{11}NO_4)_{0.239}(C_{18}H_{23}ClN_3O_5)_{0.518}$: C, 51.99; H, 6.08; N, 9.72. Found for ILCSB**1** (DS = 51.8%) C, 52.35; H, 6.33; N, 9.92 (Table 1).

On the basis of elemental and spectral analyses for ILCSBs (**1–6**) suggested structure for ILs-functionalized salicylidene chitosan architectures for the monomeric building unit is given in Scheme 4.

FTIR

Emerging or new bands coupled with marked changes in the FTIR signatures of (ILCSB**1–6**) compared with those of CS (Fig. 3) demonstrated that IL-based salicylaldehydes have been successfully grafted onto the chitosan backbone to obtain the IL-functionalized CS Schiff bases. The FTIR spectra of (ILCSB**1–6**) are quite similar. Extremely strong broad peaks around 3436 cm^{-1} arises from three overlapping peaks; phenolic O–H stretch (coincident with the maxima of aryl-O vibration bands at *ca.* 1285 cm^{-1}), amide NH stretch mode (coupled with amide I stretch around 1660 cm^{-1}) and primary amine N–H stretch (further confirmed by bending vibration shoulders of NH_2 at *ca.* 1595 cm^{-1}). Permanence of very weak

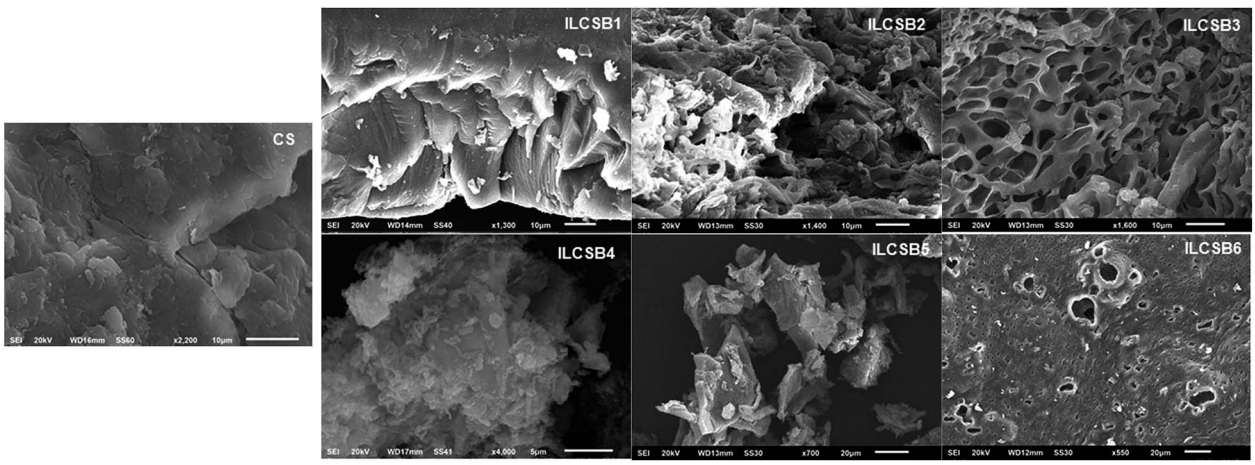

Fig. 4 Representative surface topography of CS and ILCSB**1–6** biopolymers by SEM.

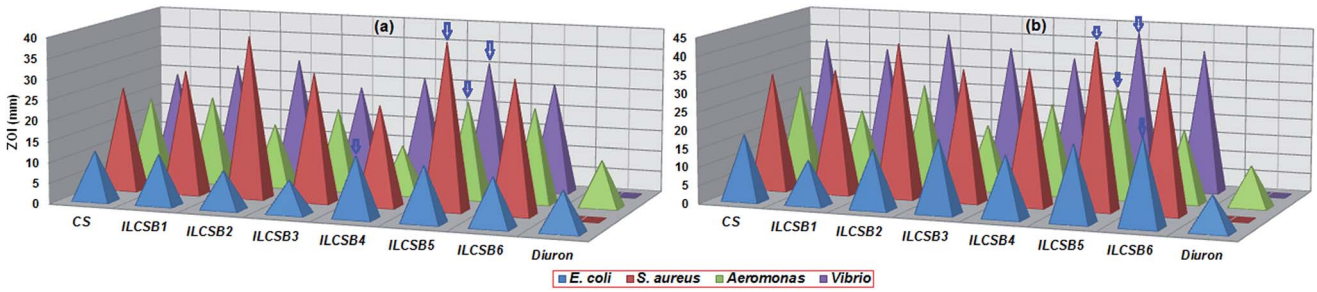

Fig. 5 Zone of inhibition (ZOI, in mm) for target compounds against different bacterial species: (a) in 40% AcOH + 40% seawater + 20% DW; (b) in 50% AcOH + 50% seawater. Arrows refer to the most potent compounds.

ν_{NH_2} shoulders confirms a decrease in $-NH_2$ group content through partial Schiff base condensation. Intense bands around 1635 cm^{-1} are due to azomethine (H–C=N) stretching vibrations which are frequently coupled or demasked with amide I stretch. Three main peaks (C=N stretching vibration: 1562–1524 cm^{-1}; PF_6^- vibrations: 845 cm^{-1} and bending vibrations: 773–757 cm^{-1}) are characteristic for the ionic liquid terminals.

NMR spectroscopy

^1H NMR spectra of (ILCSB**1–6**) have a common deshielded resonance at δ = ~10.35 ppm originating from the intramolecularly H-bonded phenolic OH,[24] and multiplets between 7.39 and 8.24 ppm assignable to aromatic protons, which confirm the successful anchoring of ILs-Sal (**2**, **3a–c**) onto the chitosan backbone. Additionally, consistent with successful surface functionalization of CS with IL-Sal is the observation of the azomethine proton signal at *ca.* 9.00 ppm. Also the intensity ratio of the anomeric proton around 4.25 ppm to that of aromatic protons at the range of 7.40–8.14 ppm clearly demonstrated that the degree of substitution[25] was around 50% which is in good agreement with the DS values calculated from elemental analysis. In the ^{13}C NMR spectra for (ILCSB**1–6**)

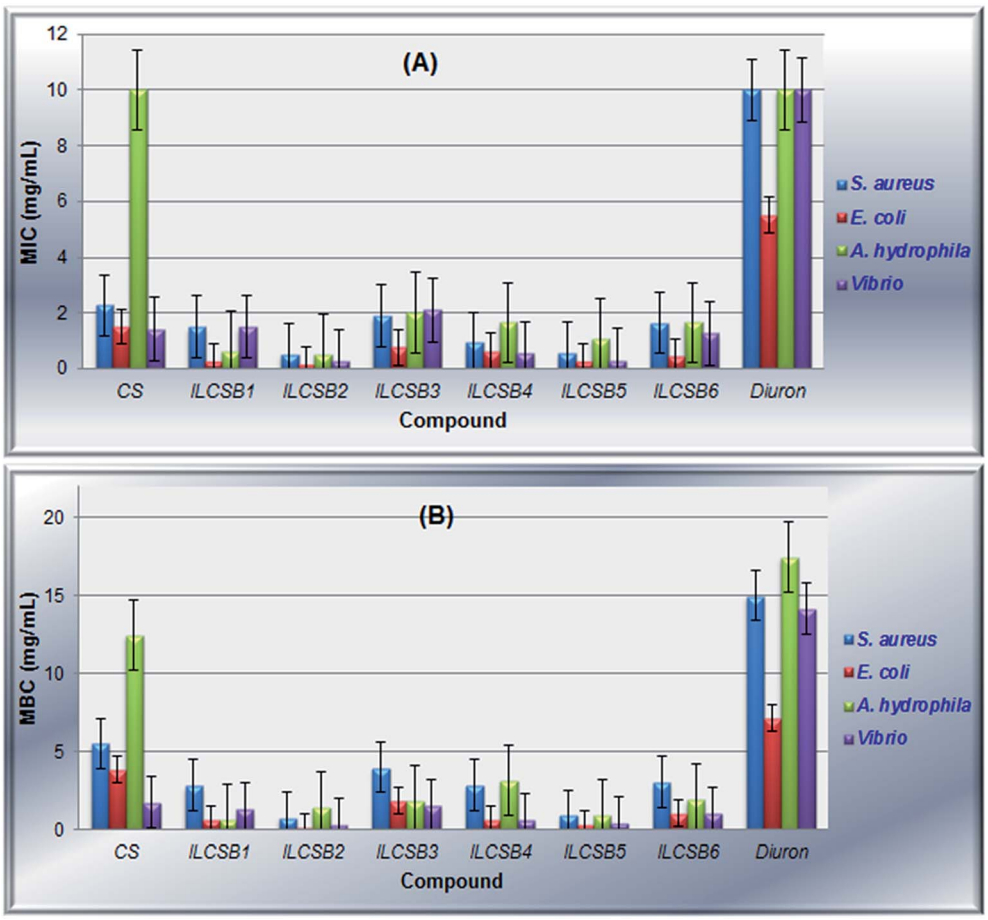

Fig. 6 Antibacterial efficacy of ILCSBs against different bacterial species in comparison to standard antifoulant, Diuron®: (A) bactericidal susceptibility (MIC); (B) bacteriostatic susceptibility (MBC).

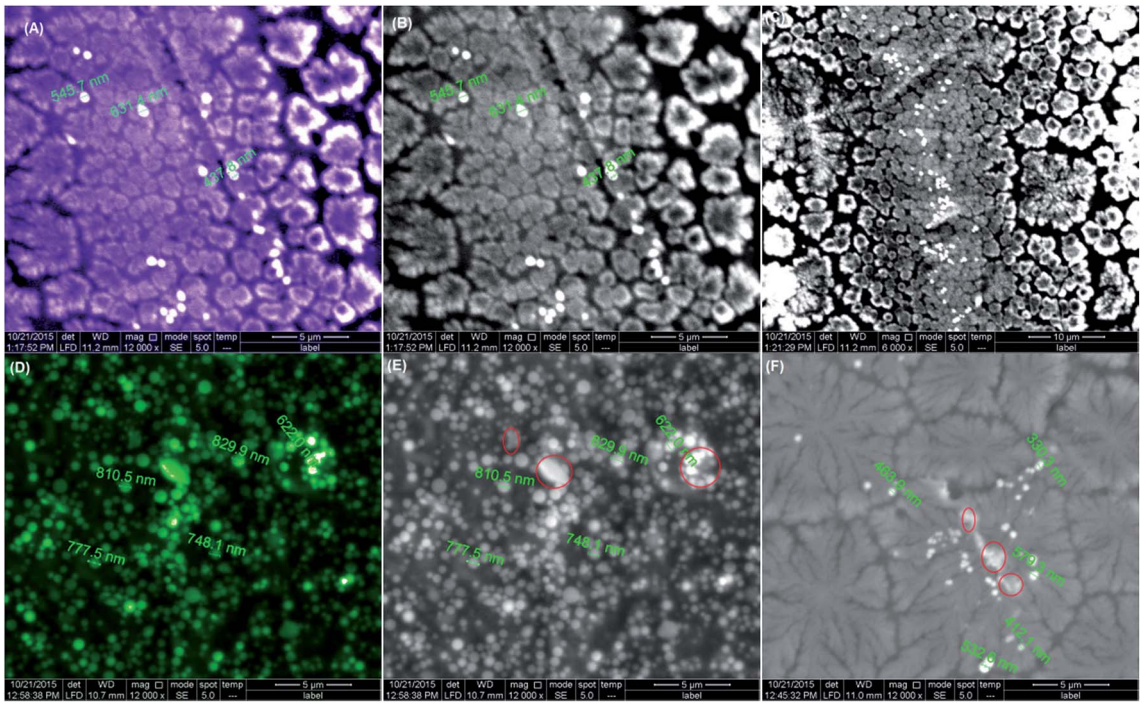

Fig. 7 SEM micrographs of both blank, control bacterial cell cultures and with ILCSB2 treated bacterial cell culture morphology. (A and B) Blank *E. coli* cells (C) control *E. coli* cells (D–F) ILCSB2 treated damaged *E. coli* cell. Red circle in SEM images shows the release of bacterial cell content after ILCSB2 antibacterial action.

signals in the range of 35–85 ppm corresponding to carbon atoms of the chitosan backbone confirm that chitosan retains its structural stability even after its chemical-modification with IL-Sal. Evidences for successful chemical anchoring of ionic liquid-factionalized salicylaldehydes to the chitosan skeleton, is provided by the set of additional peaks observed in the low field region, 107–135 ppm, attributed to the aromatic carbon atoms of salicylidene. Signals for the C–OH and HC=N carbon atoms were observed around 156 ppm and 167 ppm, respectively. Hexafluorophosphate surface-functionalization of CS in (ILCSB**4–6**) was authenticated by the appearance of the septet signal (centered at *ca.* 144 ppm) and doublet signal (centered at *ca.* 70 ppm) in their $^{31}P/^{19}F$ NMR spectra which are characteristic for PF_6^- counter anions.

Morphological and topographical characterizations of CS and ILCSBs

The self-standing ILCSB flexible films were analyzed by scanning electron microscopy (SEM) measurements (see Fig. 4), which revealed difference in the surface morphology as compared to chitosan (CS). The chitosan film surface displays a smooth, dense and flat morphology while ILCSBs exhibit rough sponge like structures.

Bacterial susceptibility profile

Many trials of new antifoulants end in failure due to the low efficacy, serious negative environmental impact or exorbitant cost for fabrication of new antifoulants. Functionalization of chitosan (CS), economically isolated from marine-waste, could provide a synergetic effect of improving biopotency/antifouling performance and at the same time may offers new generation of eco-friendly antibiofoulants.

Antibacterial activity profile. The target imidazolium/ammonium/pyridinium IL-bearing chitosan Schiff bases (ILCSBs) and a standard antifoulant, Diuron®, were *in vitro* assessed for their capacity to inhibit the growth of a range of significant biofilm-inducing bacterial strains including *Escherichia coli* (*E. coli*, ATCC 25922), *Staphylococcus aureus* (*S. aureus*, ATCC 25923), *Aeromonas hydrophila* (*A. hydrophila*) as well *Vibrio*. Generally, zone of inhibition (ZOI) data (Fig. 5) demonstrate that chitosan is a better bactericide than Diuron®, especially against *S. aureus* and *Vibrio*, which have an extraordinary capacity to attach to implanted medical devices, forming serious biofilm, through direct interaction with the device's polymer surface or by establishing adhesion to human matrix proteins that covered the device.[26] Enhanced biopotency effect can be observed by some ILCSBs in comparison to CS. This can be attributed to several reasons. Firstly, hydrogen-bonding through the azomethine group (H–C=N), H-bond acceptors, and phenolic OH, H-bond donor/acceptor, of chitosan-*N*-salicylidene fragments with the active centers of the bacterial cell constituents resulting in the interference with normal cell process.[27] Secondly, the poly(ionic liquid) brushes on the surface of chitosan can provide effective bactericidal efficacy through a contact mechanism, where, after the bacterial strains are adsorbed on the biopolymer surface by electrostatic or hydrophobic interaction, or both.[28] Cationic imidazolium,

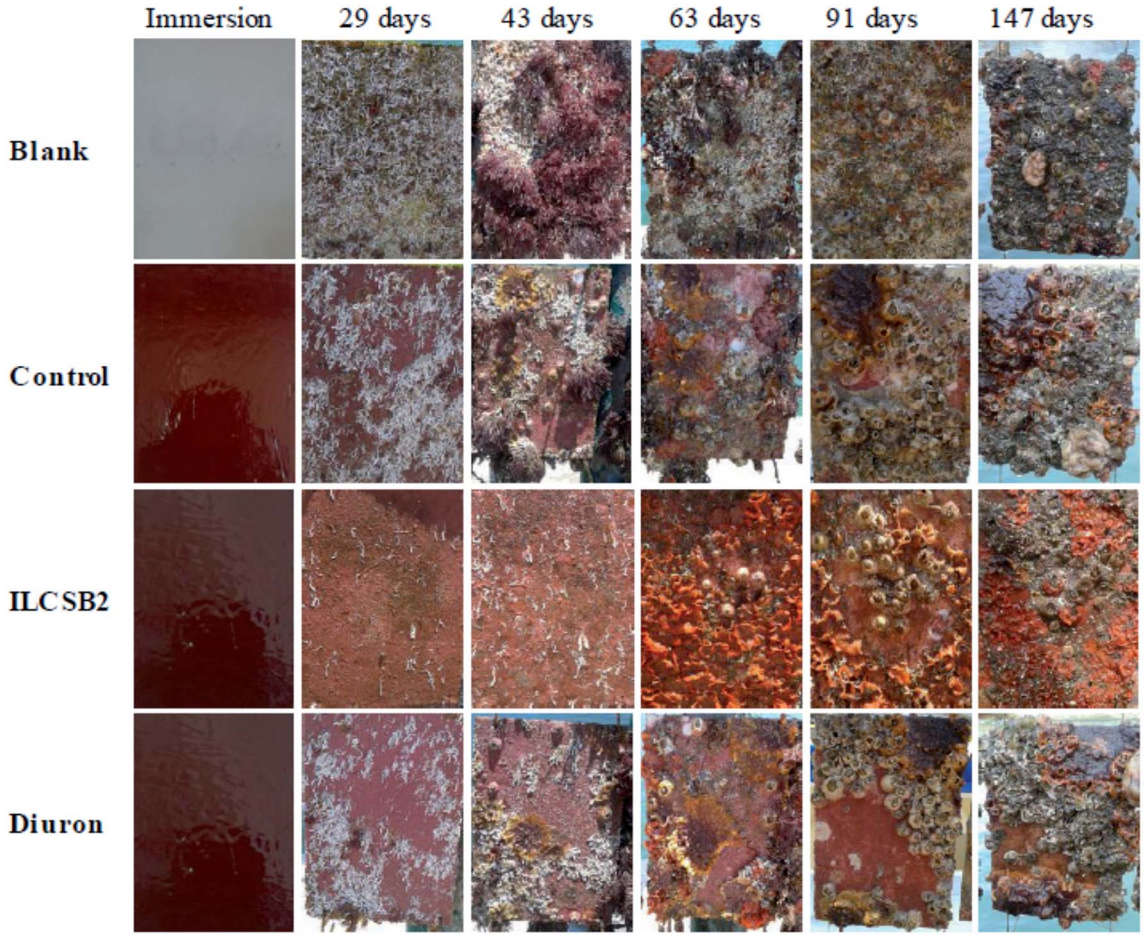

Fig. 8 Photographs collected from field test of anti-macrobiofouling assay for ILCSB2-pigment coated acrylic panels in comparison to control, Diuron-coated panels and uncoated panel (blank).

ammonium or pyridinium Sal-IL groups in the structure of poly-(GlcNHAc-GlcNH$_2$-GlcNSal-IL$^+$X$^-$) brushes enhance the antibacterial activity, due to electrostatic interactions with the negatively charged outer wall of the bacteria.[29] The hydrophobic pharmacophores (alkyl terminals) help the ionic liquids to penetrate into the bacterial cell wall and disrupt the cytoplasmic membrane with simultaneous release of potassium and other constituents, eventually causing pathogen death. Finally, the effectiveness of the ILCSBs against different pathogens depends on the permeability of the cell wall of bacterial strains which is affected by hydrophobicity–hydrophilicity balance of the target compound or difference in ribosome of the microbial cells.[30]

Among all tested compounds, ILCSB**5**, 5-(*N*,*N*,*N*-triethylammonium hexafluorophosphates)-salicylidene chitosan, exhibits remarkable extra-potent bactericidal activity in comparison to standard antifoulant, Diuron®, and can be classified as a new promising candidate to hinder attachment, colonization and growth of *Staphylococcal* and *Vibrio* strains.

Antibacterial efficacy. To compare the antibacterial efficacy of the ILCSBs, the MIC/MBC (MIC = Minimal Inhibitory Concentration; MBC = Minimal Bactericidal Concentration) were determined against tested biofouling-inducing bacteria using the macro-dilution broth susceptibility test. The results are summarized in Fig. 6 and Table S1 (see ESI†). MBC values were varied in several orders of magnitude from the MIC values, with maximum biocidal action being achieved for ILCSB**2** against *E. coli* (MIC/MBC$_{E.\ coli}$ = 0.16/0.17 mg mL^{-1}) which is 3-fold lower than that against *S. aureus* (MIC/MBC$_{S.\ aureus}$ = 0.50/0.75). The MIC and MBC values of ILCSBs were significantly lower than those of the CS and standard antifoulant, Diuron®, and varied dependent on bacterial strain, cationic core and anionic counterion. For example, it was shown that the MIC/MBC of ILCSB**5** against two different species *E. coli* and *A. hydrophila* differ by a factor of 5/6. Also, *S. aureus* viability (bactericidal effects, ΔMIC = 1.39 mg mL^{-1}) is less affected by the change of cationic/anionic sites than growth inhibition (bacteriostatic effects ΔMIC = 2.28 mg mL^{-1}). Noteworthy, the cationic core-dependent antibacterial activity of ILCSBs against *E. coli* follows the following trend: ammonium (MIC/MBC = 0.16–0.25/0.17–0.32) > imidazolium (MIC/MBC = 0.25–0.62/0.64–0.65) > pyridinium (MIC/MBC = 0.45–0.75/1.01–1.88). Furthermore, hexafluorophosphates were found to be more effective than chloride analogues as revealed by MIC/MBC data.

Preliminary anti-biofouling assay

Biofilm formation. Biofilm formation is the initial step of the complex biofouling process enables bacteria to grow under

harsh conditions and decreases their susceptibility to antibacterial/antibiofouling agents. Among biofilm-inducing bacterium, *E. coli*-dominated heterogeneous biofilm led to formation of differential aeration cells, ascribed to the differences in oxygen levels between the biofilm-coated and the area exposed to the environment,[31] which in turn triggers pitting corrosion. Therefore, extensive research efforts have been devoted to fight and prevent attachment, colonization and biofilm growth due to bacterial attack. Yet, control and eradication of biofilms are difficult since their resistance toward most antibiofoulants and biocides is substantially increased.[32] The effectiveness of most efficient biocidal ILs-functionalized CS, ILCSB**2**, in inhibiting *E. coli*-biofilm formation was investigated by scanning electron microscopy (SEM). On comparing the morphology of the blank (Fig. 7A and B) and control bacterial strains (Fig. 7C) with that treated with solution of ILCSB**2** (Fig. 7D–F), it was noticed that; (i) the *E. coli* cells were not aggregated in clusters as in the blank and control. (ii) The blank and control slides exhibited well developed dense *E. coli* biofilm growth which reduced considerably ILCSB**2**-treated *E. coli* cells. (iii) The cellular morphology of a portion of ILCSB**2**-treated *E. coli* has significantly changed such as shrinkage of *E. coli* cells due to partial damage to the cell membrane (*cf.* Fig. 7D–F). The consequences of damaged cell membrane integrity might be due to the creation of numerous of membrane pores, as a result of ILCSB**2** penetration, prompting leakage of cytoplasmic contents and accumulation of cell debris (red circle in Fig. 7E and F). These results confirm that the poly-(GlcNSal-MeIm^{+}Cl^{-}) brushes can efficiently inhibit *E. coli* biofilm-growth and kill most of the *E. coli* cells on the CS surface.

Field antibiofouling trial in the marine environment. ILCSB**2**-pigment coated acrylic panel was submerged in a natural marine environment to investigate the biofouling propensity of this coating, in comparison to blank, pigment and standard antifoulant (Diuron®) coated panels, at Alexandria Eastern Harbor beach in Egypt for 147 days. Evidence of macrofouling by attachment of macroorganisms is observed by visual inspection. Fig. 8 shows the appearance of different coated/uncoated panels with time intervals for 147 days, data were collected in Table S2 (see ESI†). There were many factors affecting brown and red algal growth during test period, among these factors temperature level and nutrients, concentration. (1) Temperature; after 91 days temperature decreased to its minimum value 21.7 °C but for both brown and red algae to grow they need more warmer water than this level, consequently adhesion of these algae is considerably decreases after 91 days. (2) Nutrients level; similarly they decreased to their minimum values from 91 to 147 days. Those nutrients are essential for brown and red algae to grow (*i.e.* they must be high enough to their growth). By comparison ILCSB**2** minimized their growth than normal (blank) during the same periods as shown in the following figures and photos. The adhesion of marine fouling macroorganisms to the surface of blank follows the following affinity trend: tube worm (100% panel coverage after 147 days) > brown macroalgae (60% panel coverage after 91 days) > barnacles (65% panel coverage after 147 days) > bryozoans (60% panel coverage after 147 days) > red macroalgae (30% panel coverage after 63 days) > green macroalgae (25% panel coverage after 147 days) > tunicates-zooids (20% panel coverage after 147 days) > ascidians (5% panel coverage after 147 days). On the other

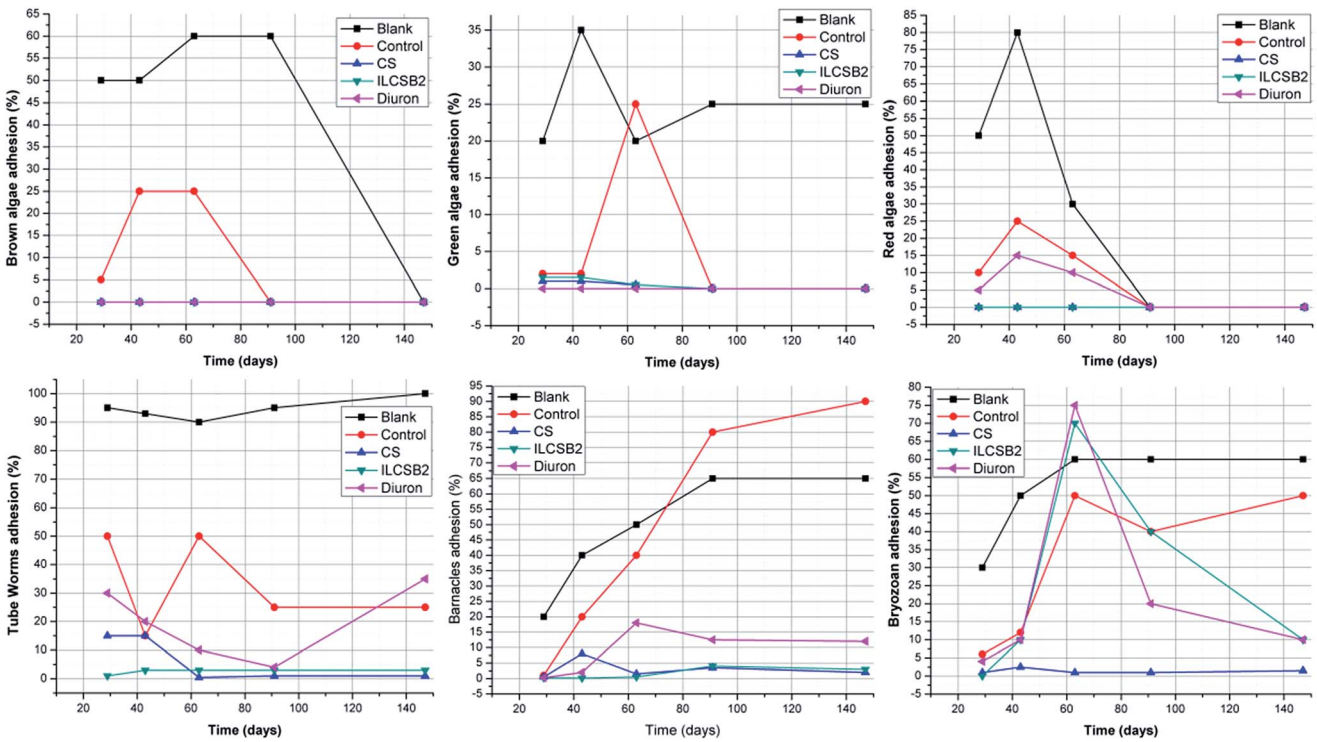

Fig. 9 Macroorganism panel coverage percent with time intervals for blank, control and painted acrylic panels immersed in Alexandria Eastern Harbor starting from (12 May 2015) to (6 October 2015).

hand, representative photographs collected for control, Diuron® and ILCSB2 coated panels showed different biofouling propensity. All settlement data showed a statistically significant reduction in macrofoulant density on coated surfaces relative to the uncoated surface (blank) (see Fig. 9). The experimental results showed that the ILCSB2-coated exhibited extraordinary resistance to adhesion of fouling organisms and prevention of biofouling where this panel seems to retain a relatively clear surface appearance throughout the period of study, yet the coating failed at the 8th week. Interestingly, the congested fouling population on ILCSB2-coated panel is lower than that of standard antifoulant (Diuron®)-coated panel as revealed from organism coverage percent where for example, ILCSB2 showed no growth of red macroalgae during immersion period (0% after 147 days) while Diuron® showed a growth of (10% after 63 days). Furthermore, lower densities of tube worms, barnacles and bryozoan were attached to the ILCSB2 panel surface when compared with the Diuron panel. From the obtained results we can concluded that ILCSB2 showed superior fouling resistance and prevention against macro-fouling of organism settlements.

Conclusion

Our work demonstrates a simple, safe, cost-effective, and eco-friendly preparation of ionic liquid brushes-functionalized chitosan-*N*-salicylidene (ILCSBs). To our knowledge, this study is the first to utilize IL-Sal in chitosan functionalization. The designed ionic liquid brushes-chitosan-*N*-salicylidenes exhibit excellent and broad antibacterial efficacy compared to parent chitosan and standard antifoulant, Diuron®, against common panel of biofilm-inducing marine bacteria such as *S. aureus*, *E. coli*, *A. hydrophila* and *Vibrio*. We have evaluated anti-biofouling properties of the most efficient biocidal ILs-functionalized CS, ILCSB2, through: (i) study its ability to inhibit the growth *E. coli*-biofilm using scanning electron microscopy (SEM). (ii) Field immersion coating study to investigate the ability of marine fouling macroorganism to attach to acrylic surface coated with antifouling paint assembled by commercial pigment incorporated with ILCSB2. The obtained data revealed that novel ionic liquid brushes-chitosan-*N*-salicylidenes surfaces exhibited good marine conditions durability and can efficiently inhibit *E. coli* biofilm-growth or kill most of the *E. coli* cells on the CS surface. Moreover, they could achieve economical savings, considering the annual costs sustained for controlling biofouling impact.

Acknowledgements

We acknowledge the financial supports of this work by STDF (STDF-STF-Cycle4-6392 and GE-SEED-6879) to RFME and by the German Academic Exchange Service (DAAD) through PPP Ägypten 14 to CJ (Project-ID 57085711). Part of this work is also funded by BMBF project OptiMat 03SF0492C to CJ.

Notes and references

1 (*a*) I. Eshet, V. Freger, R. Kasher, M. Herzberg, J. Lei and M. Ulbricht, *Biomacromolecules*, 2011, **12**, 2681–2685; (*b*) Q. Liu, A. Singh and L. Liu, *Biomacromolecules*, 2013, **14**, 226–231; (*c*) S. Krishnan, C. J. Weinman and C. K. Ober, *J. Mater. Chem.*, 2008, **18**, 3405–3413.

2 L. D. Chambers, K. R. Stokes, F. C. Walsh and R. J. K. Wood, *Surf. Coat. Technol.*, 2006, **201**, 362–365.

3 (*a*) S. Hou, E. A. Burton, K. A. Simon, D. Blodgett, Y.-Y. Luk and D. Ren, *Appl. Environ. Microbiol.*, 2007, **73**, 4300–4307; (*b*) S. Schlag, C. Nerz, T. A. Birkenstock, F. Altenberend and F. Gotz, *J. Bacteriol.*, 2007, **189**, 7911–7919; (*c*) Y. F. Zhu, E. C. Weiss, M. Otto, P. D. Fey, M. S. Smeltzer and G. A. Somerville, *Infect. Immun.*, 2007, **75**, 4219–4226.

4 (*a*) N. J. Shikuma and M. G. Hadfield, *Biofouling*, 2010, **26**, 39–46; (*b*) S. Rajalakshmi, A. Fathima, J. R. Rao and B. U. Nair, *RSC Adv.*, 2014, **4**, 32004–32012.

5 (*a*) S. Prakash, R. Ramasubburayan, P. Iyapparaj, A. Perumal, R. Arthi, N. K. Ahila, V. S. Ramkumar, G. Immanuel and A. Palavesamb, *RSC Adv.*, 2015, **5**, 29524–29534; (*b*) J. Muralidharan and S. Jayachandran, *Process Biochem.*, 2003, **38**, 841–847.

6 S. Krishnan, C. J. Weinman and C. K. Ober, *J. Mater. Chem.*, 2008, **18**, 3405–3413.

7 (*a*) N. Fusetani, *Nat. Prod. Rep.*, 2011, **28**, 400–410; (*b*) Y. T. Cui, S. L. Teo, W. Leong and C. L. Chai, *Int. J. Mol. Sci.*, 2014, **15**, 9255–9284.

8 (*a*) H. K. No, N. Y. Park, S. H. Lee and S. P. Meyers, *Int. J. Food Microbiol.*, 2002, **74**, 65–72; (*b*) S. Roller and N. Covill, *Int. J. Food Microbiol.*, 1999, **47**, 67–77; (*c*) J. Rhoades and S. Roller, *Appl. Environ. Microbiol.*, 2000, **66**(1), 80–86; (*d*) N. R. Sudarshan, D. G. Hoover and D. Knorr, *Food Biotechnol.*, 1992, **6**(3), 257–272; (*e*) B. K. Choi, K. Y. Kim, Y. J. Yoo, S. J. Oh, J. H. Choi and C. Y. Kim, *Int. J. Antimicrob. Agents*, 2001, **18**(6), 553–557.

9 I. L. Roux, H. M. Krieg, C. A. Yeates and J. C. Breytenbach, *J. Membr. Sci.*, 2005, **248**, 127–136.

10 G. Sauvet, W. Fortuniak, K. Kazmierski and J. Chojnowski, *J. Polym. Sci., Part A: Polym. Chem.*, 2003, **41**, 2939–2948.

11 (*a*) B. Gottenbos, H. C. van der Mei, F. Klatter, P. Nieuwenhuis and H. J. Busscher, *Biomaterials*, 2002, **23**, 1417–1423; (*b*) J. Hazzizalaskar, N. Nurdin, G. Helary and G. Sauvet, *J. Appl. Polym. Sci.*, 1993, **50**, 651–662.

12 (*a*) R. F. M. Elshaarawy and C. Janiak, *Tetrahedron*, 2014, **70**, 8023–8032; (*b*) R. F. M. Elshaarawy, Z. H. Kheiralla, A. A. Rushdy and C. Janiak, *Inorg. Chim. Acta*, 2014, **421**, 110–122; (*c*) R. F. M. Elshaarawy and C. Janiak, *Eur. J. Med. Chem.*, 2014, **75**, 31–42; (*d*) L. Carson, P. K. W. Chau, M. J. Earle, M. A. Gilea, B. F. Gilmore, S. P. Gorman, M. T. McCann and K. R. Seddon, *Green Chem.*, 2009, **11**, 492–497; (*e*) K. M. Docherty and J. C. F. Kulpa, *Green Chem.*, 2005, **7**, 185–189.

13 (*a*) E. E. Alberto, L. L. Rossato, S. H. Alves, D. Alves and A. L. Braga, *Org. Biomol. Chem.*, 2011, **9**, 1001–1003; (*b*) J. Pernak, K. Sobaszkiewicz and I. Mirska, *Green Chem.*, 2003, **5**, 52–56.

14 H. Nakajima and H. Ohno, *Polymer*, 2005, **46**, 11499–11504.

15 O. Azzaroni, S. Moya, T. Farhan, A. A. Brown and W. T. S. Huck, *Macromolecules*, 2005, **38**, 10192–10199.

16 J. Lu, F. Yan and J. Texter, *Prog. Polym. Sci.*, 2009, **34**, 431–448.
17 W. Jia, Y. Wu, J. Huang, Q. An, D. Xu, Y. Wu, F. Li and G. Li, *J. Mater. Chem.*, 2010, **20**, 8617–8623.
18 (*a*) R. F. M. Elshaarawy, T. B. Mostafa, A. A. Refaee and E. A. El-Sawi, *RSC Adv.*, 2015, **5**, 68260–68269; (*b*) R. F. M. Elshaarawy and C. Janiak, *Arabian J. Chem.*, 2015, DOI: 10.1016/j.arabjc.2015.04.010; (*c*) H. K. Ibrahim, E. Eltamany, R. F. M. Elshaarawy and I. Mohy-Eldeen, *Maced. J. Chem. Chem. Eng.*, 2008, **27**(1), 65–79.
19 A. Percot, C. Viton and A. Domard, *Biomacromolecules*, 2003, **4**(1), 12–18.
20 C. Perez and P. Bazerque, *Acta Biol. Med. Exp.*, 1990, **15**, 113–115.
21 X. Hu, Y. Du, Y. Tang, Q. Wang, T. Feng, J. Yang and J. F. Kennedy, *Carbohydr. Polym.*, 2007, **70**, 451–458.
22 M. R. Kasaai, *Carbohydr. Polym.*, 2008, **71**, 497–508.
23 (*a*) M. Lavertu, Z. Xia, A. N. Serreqi, M. Berrada, A. Rodrrigues, D. Wang, M. D. Buschmann and A. Gupta, *J. Pharm. Biomed. Anal.*, 2003, **32**, 1149–1158; (*b*) Y. Shigemasa, H. Matsuura, H. Sashiwa and H. Saimato, *Int. J. Biol. Macromol.*, 1996, **18**, 237–242.
24 Y. S. Zhou, L. J. Zhang, X. R. Zeng, J. J. Vital and X. Z. You, *J. Mol. Struct.*, 2000, **553**, 25–30.
25 R. S. Jagadish, K. N. Divyashree, P. Viswanath, P. Srinivas and B. Raja, *Carbohydr. Polym.*, 2012, **87**, 110–116.
26 (*a*) M. Otto, *Curr. Top. Microbiol. Immunol.*, 2008, **322**, 207–228; (*b*) H. Y. Fitnat and K. L. Visick, *Trends Microbiol.*, 2009, **17**, 109–118.
27 R. Prabhakaran, A. Geetha, M. Thilagavathi, R. Karvembu, V. Krishnan, H. Bertagnolli and K. Natarajan, *J. Inorg. Biochem.*, 2004, **98**, 2131–2140.
28 Y. Nakagawa, H. Hayashi, T. Tawaratani, H. Kourai, T. Horie and I. Shibasaki, *Appl. Environ. Microbiol.*, 1984, **47**, 513–518.
29 F. Baudrion, A. Périchaud and E. Vacelet, *Biofouling*, 2000, **14**, 317–331.
30 P. G. Lawrence, P. L. Harold and O. G. Francis, *Antibiot. Chemother.*, 1957, **4**, 1980–1989.
31 R. J. Zuo and T. K. Wood, *Appl. Microbiol. Biotechnol.*, 2004, **65**, 747–753.
32 T. R. de Kievit, M. D. Parkins, R. J. Gillis, R. Srikumar, H. Ceri, K. Poole, B. H. Iglewski and D. G. Storey, *Antimicrob. Agents Chemother.*, 2001, **45**, 1761–1770.